NJC

PAPER

View Article Online
View Journal | View Issue

Cite this: *New J. Chem.*, 2014, **38**, 2587

A single chemosensor for multiple analytes: fluorogenic detection of Zn^{2+} and OAc^- ions in aqueous solution, and an application to bioimaging†

Gyeong Jin Park,[a] Yu Jeong Na,[a] Hyun Yong Jo,[a] Seul Ah Lee,[a] Ah Ram Kim,[b] Insup Noh[b] and Cheal Kim*[a]

Received (in Montpellier, France) 7th February 2014,
Accepted 17th March 2014

DOI: 10.1039/c4nj00191e

www.rsc.org/njc

A new highly selective and sensitive chemosensor **1** for both Zn^{2+} and OAc^- with off–on fluorescence behavior in aqueous solution was developed. The selectivity mechanism of **1** for zinc is based on a combinational effect of the inhibition of excited-state intramolecular proton transfer and C=N isomerization, and chelation-enhanced fluorescence. As a practical application, *in vitro* studies with fibroblasts showed fluorescence in the presence of both the receptor **1** and Zn^{2+}. Moreover, the deprotonated **1** can behave as a chemosensing system for turn-on detection of OAc^- in preference over various other anions tested. Therefore, **1** can serve as 'one sensor for multiple analytes'.

Introduction

Development of chemical probes for the sensing of metal ions[1] and anions[2] has received considerable attention due to their fundamental applications in chemical, environmental and biological fields. For *e.g.*, despite the fact that zinc has significant roles in catalytic centers and structural cofactors of many Zn^{2+}-containing enzymes and DNA-binding proteins,[3] an unregulated zinc level in the body may lead to a number of severe neurological diseases (*e.g.* Alzheimer's disease, cerebral ischemia, and epilepsy), developmental defects, and malfunctions.[4] Therefore, considerable effort has been devoted to the development of efficient and selective methods to detect Zn^{2+}.[4b]

Among the anionic species, the acetate ion (OAc^-) has received the most attention because it is a major component of numerous metabolic processes.[5] The rate of OAc^- production and oxidation has been frequently used as an indicator of organic decomposition in marine sediments.[5b,c] Thus, detection of OAc^- in a trace amount is important not only for a biological process, but also for environmental applications.[6]

Numerous approaches, such as inductively coupled plasma atomic emission spectrometry,[7] atomic absorption spectroscopy,[8] and electrochemical methods,[9] have been employed to detect both the metal ions and anions. However, most of these methods require sophisticated instrumentations, tedious sample preparation procedures, and trained operators. By contrast, fluorescence technology provides a convenient and an easy monitoring of the target ions.[10] Detection methods using fluorescence have, therefore, attracted considerable attention in the detection of metal ions or anions, including Zn^{2+} and OAc^-.

Recently, single chemosensors for multiple analytes have become very popular among the analysts, because of their fast detection time and cost reduction. Examples of such sensors are Zn^{2+}/F^-,[11a] Cu^{2+}/F^-,[11a] Zn^{2+}/H_2O_2,[11b] Zn^{2+}/HSO_4^-,[11c] Zn^{2+}/S^{2-},[11d] and Cu^{2+}/S^{2-}.[11e]

Herein this paper, we report the synthesis and sensing properties of a new imine-based chemosensor **1**, which has both an amide and an imine functional group. Our approach to design this fluorescence based bi-functional chemosensor relies on the strong coordination power of a Schiff base (imine) to metal ions and the possibility of a hydrogen bond between the amide (CONH)/OH groups and the targeted anions. Receptor **1** showed an intense fluorescence enhancement in the presence of zinc ions in aqueous solution, and sensed Zn^{2+} ions in the cells for application to bioimaging. Additionally, **1** could also detect acetate ions in aqueous solution through an enhancement of emission with high selectivity and sensitivity.

Experimental section

General information

All the solvents and reagents (analytical grade and spectroscopic grade) were obtained from Sigma-Aldrich and used as

[a] *Department of Fine Chemistry and Department of Interdisciplinary Bio IT Materials, Seoul National University of Science and Technology, Seoul 139-743, Korea. E-mail: chealkim@seoultech.ac.kr; Fax: +82-2-973-9149; Tel: +82-2-970-6693*

[b] *Department of Chemical Engineering, Seoul National University of Science & Technology, Seoul 139-743, Korea*

† Electronic supplementary information (ESI) available. See DOI: 10.1039/c4nj00191e

received. ^{1}H NMR and ^{13}C NMR measurements were performed on a Varian 400 MHz spectrometer and chemical shifts are recorded in ppm. Electrospray ionization mass spectra (ESI-MS) were collected on a Thermo Finnigan (San Jose, CA, USA) LCQTM Advantage MAX quadruple ion trap instrument. Elemental analysis of carbon, nitrogen, and hydrogen was carried out by using a Flash EA 1112 elemental analyzer (thermo) in Organic Chemistry Research Center of Sogang University, Korea. UV-vis spectra were recorded at room temperature using a Perkin Elmer model Lambda 2S UV/Vis spectrometer. Fluorescence measurements were performed on a Perkin Elmer model LS45 fluorescence spectrometer.

Synthesis of receptor 1

3-Hydroxy-2-naphthoic hydrazide (0.20 g, 1 mmol) was dissolved in 30 mL of ethanol, and 8-hydroxyjulolidine-9-carboxaldehyde (0.26 g, 1.2 mmol) was added into the solution over 10 minutes. The reaction mixture was stirred for 4 h at room temperature until a dark yellow precipitate appeared. The resulting precipitate was filtered and washed 2 times with diethyl ether. The yield: 0.35 g (87%). ^{1}H NMR (dimethyl sulfoxide (DMSO)-d_6, 400 MHz) δ: 12.59 (s, 1H), 12.35 (s, 1H), 12.04 (s, 1H), 9.08 (s, 1H), 8.99 (s, 1H), 8.54 (d, 1H), 8.39 (d, 1H), 8.15 (d, 1H), 8.00 (d, 1H), 7.95 (s, 1H), 7.39 (s, 1H), 3.82 (m, 4H), 3.26 (m, 4H), 2.49 (m, 4H). ^{13}C NMR (DMSO-d_6, 400 MHz) δ: 162.96, 154.77, 154.37, 151.67, 145.44, 135.84, 129.82, 128.62, 128.44, 128.20, 126.71, 125.83, 123.77, 119.45, 112.53, 110.60, 106.22, 105.61, 49.31, 48.85, 26.53, 21.47, 20.64, 20.19 ppm. HRMS (ESI): m/z calcd for $C_{24}H_{23}N_3O_3 + H^+$: 402.18 [M + H$^+$]: found, 402.16. Anal. calcd for $C_{24}H_{23}N_3O_3$ (401.46): C, 71.80; H, 5.77; N, 10.47. Found: C, 71.61; H, 5.36; N, 10.69%.

Physical properties, NMR titration and cell imaging of receptor 1 with zinc ions

UV-vis measurements. Receptor **1** (0.60 mg, 0.0015 mmol) was dissolved in dimethylformamide (DMF) (0.5 mL) and 10 μL of the receptor **1** (3 mM) were diluted to 2.990 mL DMF/bis-tris buffer solution (v/v = 1 : 1) to make the final concentration of 10 μM. $Zn(NO_3)_2{\cdot}6H_2O$ (30.0 mg, 0.1 mmol) was dissolved in DMF (5 mL). 1.5–15 μL of the Zn^{2+} solution (20 mM) were transferred to each receptor solution (10 μM) prepared above. After mixing them for a few seconds, UV-vis absorption spectra were taken at room temperature.

Fluorescence measurements. Receptor **1** (0.60 mg, 0.0015 mmol) was dissolved in DMF (0.5 mL) and 10 μL of the receptor **1** (3 mM) were diluted in 2.990 mL DMF/bis-tris buffer solution (v/v = 1 : 1) to make the final concentration of 10 μM. $Zn(NO_3)_2{\cdot}6H_2O$ (30.0 mg, 0.1 mmol) was dissolved in DMF (5 mL). 1.5–22.5 μL of the Zn^{2+} solution (20 mM) were transferred to each receptor solution (10 μM) prepared above. After mixing them for a few seconds, fluorescence spectra were obtained at room temperature.

Competition with other metal ions. Receptor **1** (0.60 mg, 0.0015 mmol) was dissolved in DMF (0.5 mL) and 10 μL of the receptor **1** (3 mM) were diluted to 2.990 mL DMF/bis-tris buffer solution (v/v = 1 : 1) to make the final concentration of 10 μM. $M(NO_3)$ (M = Na, K, 0.1 mmol), $M(NO_3)_2$ (M = Mn, Co, Ni, Cu, Zn, Cd, Hg, Mg, Ca, Pb, 0.1 mmol), $M(ClO_3)_2$ (M = Fe, 0.1 mmol) or $M(NO_3)_3$ (M = Al, Cr, 0.1 mmol) were dissolved in DMF (5 mL), respectively. 22.5 μL of each metal solution (20 mM) were taken and added into 3 mL of each receptor **1** solution (10 μM) prepared above to make 15 equiv. Then, 22.5 μL of the $Zn(NO_3)_2$ solution (20 mM) were added into the mixed solution of each metal ion and receptor **1** to make 10 equiv. After mixing them for a minute, fluorescence spectra were taken at room temperature.

Job plot measurement. Receptor **1** (0.60 mg, 0.0015 mmol) was dissolved in DMF (0.5 mL). 12, 10.8, 9.6, 8.4, 7.2, 6.0, 4.8, 3.6, 2.4, and 1.2 μL of the receptor **1** solution were taken and transferred to vials. Each vial was diluted with DMF to make a total volume of 2.988 mL. $Zn(NO_3)_2{\cdot}6H_2O$ (0.45 mg, 0.0015 mmol) was dissolved in DMF (0.5 mL). 0, 1.2, 2.4, 3.6, 4.8, 6.0, 7.2, 8.4, 9.6, 10.8, and 12 μL of the $Zn(NO_3)_2$ solution were added to each diluted receptor **1** solution. Each vial had a total volume of 3 mL. After shaking the vials for a few minutes, fluorescence spectra were taken at room temperature.

NMR titration. For ^{1}H NMR titrations of receptor **1** with Zn^{2+}, four NMR tubes of receptor **1** (2.01 mg, 0.005 mmol) dissolved in DMSO-d_6 (300 μL) were prepared and then four different concentrations (0, 0.0015, 0.0025 and 0.005 mmol) of $Zn(NO_3)_2{\cdot}6H_2O$ dissolved in DMSO-d_6 were added to each solution of receptor **1**. After shaking them for a minute, ^{1}H NMR spectra were taken at room temperature.

Methods for cell imaging. Human dermal fibroblast cells in low passage were cultured in FGM-2 medium (Lonza, Switzerland) supplemented with 10% fetal bovine serum, 1% penicillin/streptomycin in the *in vitro* incubator with 5% CO_2 at 37 °C. Cells were seeded onto a 12 well plate (SPL Lifesciences, Korea) at a density of 2×10^5 cells per well and then incubated at 37 °C for 4 h after addition of various concentrations (0–50 μM) of $Zn(NO_3)_2$. After washing with phosphate buffered saline (PBS) two times to remove the remaining $Zn(NO_3)_2$, the cells were incubated with **1** (20 μM) at room temperature for 30 min. The cells were observed using a microscope (Olympus, Japan). The fluorescent images of the cells were obtained using a fluorescence microscope (Leica DMLB, Germany) at an excitation wavelength of 515–560 nm.

Physical properties, NMR titration and UV-vis measurements of receptor 1 with acetate

UV-vis measurements. Receptor **1** (0.60 mg, 0.0015 mmol) was dissolved in DMF (0.5 mL) and 10 μL of the receptor **1** (3 mM) were diluted to 2.990 mL DMF/bis-tris buffer solution (v/v = 7 : 3) to make the final concentration of 10 μM. Tetrabutyl ammonium (TBA) acetate (162 mg, 0.5 mmol) was dissolved in DMF (5 mL). 3–30 μL of the acetate solution (100 mM) were transferred to each receptor solution (10 μM) prepared above. After mixing them for a few seconds, UV-vis absorption spectra were taken at room temperature.

Fluorescence measurements. Receptor **1** (0.60 mg, 0.015 mmol) was dissolved in DMF (0.5 mL) and 10 μL of the receptor **1** (3 mM) were diluted with 2.990 mL DMF/bis-tris buffer solution (v/v = 7 : 3) to make the final concentration of 10 μM. (TBA) acetate (162 mg, 0.5 mmol) was dissolved in DMF (5 mL). 3–30 μL of the acetate solution (100 mM) were transferred to each receptor

solution (10 μM) prepared above. After mixing them for a few minutes, fluorescence spectra were obtained at room temperature.

Competition with other metal ions. Receptor **1** (0.60 mg, 0.0015 mmol) was dissolved in DMF (0.5 mL) and 10 μL of the receptor **1** (3 mM) were diluted to 2.990 mL DMF/bis-tris buffer solution (v/v = 7 : 3) to make the final concentration of 10 μM. Tetraethyl ammonium (TEA) X (X = F, Cl, Br, I, CN, H_2PO_4, 0.5 mmol), (TBA) X (X = OAc^-) and NaX (X = N_3^-) were dissolved in DMF (5 mL), respectively. 30 μL of each anion solution (100 mM) were taken and added into 3 mL of each receptor **1** solution (10 μM) prepared above to make 100 equiv. Then, 30 μL of acetate solution (100 mM) were added into the mixed solution of each metal ion and receptor **1** to make 100 equiv. After mixing them for a few minutes, fluorescence spectra were taken at room temperature.

Job plot measurement. Receptor **1** (0.60 mg, 0.015 mmol) was dissolved in DMF (0.5 mL). 12, 10.8, 9.6, 8.4, 7.2, 6.0, 4.8, 3.6, 2.4, and 1.2 μL of the receptor **1** solution were taken and transferred to vials. Each vial was diluted with DMF to make a total volume of 2.988 mL. (TBA) acetate (4.86 mg, 0.015 mmol) was dissolved in DMF (0.5 mL). 0, 1.2, 2.4, 3.6, 4.8, 6.0, 7.2, 8.4, 9.6, 10.8, and 12 μL of the acetate solution were added to each diluted receptor **1** solution. Each vial had a total volume of 3 mL. After shaking the vials for a few minutes, fluorescence spectra were taken at room temperature.

NMR titration. For ^{1}H NMR titrations of receptor **1** with acetate, three NMR tubes of receptor **1** (2.01 mg, 0.005 mmol) dissolved in DMF-d_7 (300 μL) were prepared and then three different concentrations (0, 0.005 and 0.01 mmol) of acetate dissolved in DMF-d_7 were added to each solution of receptor **1**. After shaking them for a minute, ^{1}H NMR spectra were taken at room temperature.

Results and discussion

The receptor **1** was obtained in high yield (87%) through coupling of 3-hydroxy-2-naphthoic hydrazide with 8-hydroxyjulolidine-9-carboxaldehyde in ethanol (Scheme 1), which was subsequently characterized by ^{1}H NMR, ^{13}C NMR, elemental analysis and ESI-mass spectrometry.

Fluorescence and absorption spectroscopic studies of 1 toward Zn^{2+} ions

To gain an insight into the fluorescent properties of receptor **1** toward metal ions, the emission changes were measured with various metal ions in bis-tris buffer solution (10 mM, pH 7.0) containing 50% DMF. When excited at 410 nm, **1** exhibited a weak fluorescence with a low quantum yield (Φ = 0.0251), which

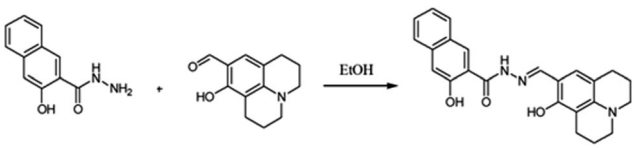

Scheme 1 Synthetic procedure of **1**.

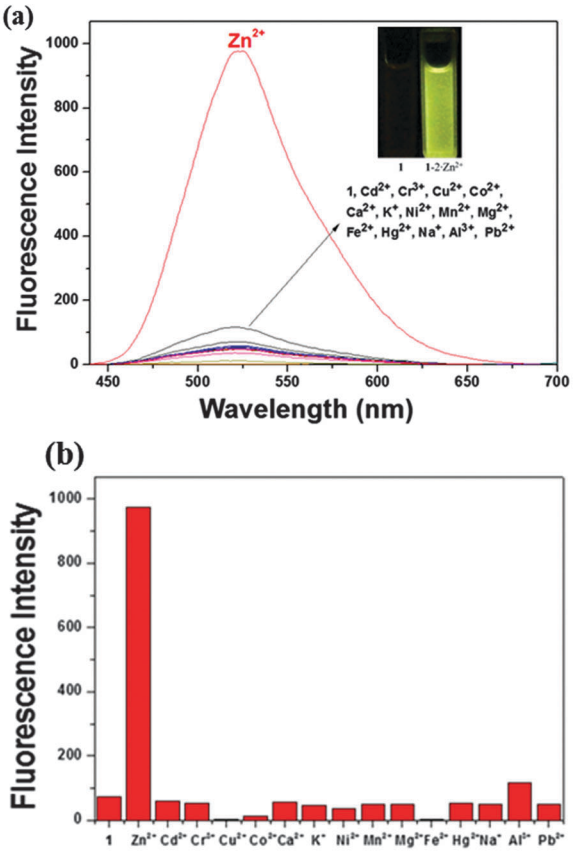

Fig. 1 (a) Fluorescence spectral changes of **1** (10 μM) in the presence of different metal ions (15 equiv.) such as Cd^{2+}, Cr^{3+}, Cu^{2+}, Co^{2+}, Ca^{2+}, K^+, Ni^{2+}, Mn^{2+}, Mg^{2+}, Fe^{2+}, Hg^{2+}, Na^+, Al^{3+}, Pb^{2+} and Zn^{2+} with an excitation of 410 nm in buffer–DMF (1 : 1, v/v). (b) Bar graph shows the relative emission intensity of **1** at 525 nm upon treatment with various metal ions.

was much lower than that (Φ = 0.222) in the presence of Zn^{2+}. By contrast, upon addition of other metal ions such as Cd^{2+}, Cr^{3+}, Cu^{2+}, Co^{2+}, Ca^{2+}, K^+, Ni^{2+}, Mn^{2+}, Mg^{2+}, Fe^{2+}, Hg^{2+}, Na^+, Al^{3+} and Pb^{2+}, either no or a slight increase in intensity was observed (Fig. 1). To this end, it is noteworthy that, **1** can act as a "turn-on" sensor for Zn^{2+} and differentiate Zn^{2+} from Cd^{2+}, which had been a major problem almost always in the past.[12] This preferential fluorescence enhancement for Zn^{2+} might be due to the formation of a chelate complex (rigid system) between **1** and the Zn^{2+} ion, leading to the chelation-enhanced fluorescence (CHEF) effect.[13] Additionally, receptor **1** is a poor fluorescent due to the combined effects: (a) isomerization of the C=N double bond in the excited state[14] and (b) excited-state intramolecular proton transfer (ESIPT), involving the phenolic protons of the julolidine moiety (Scheme 2).[15] Upon stable chelation with the zinc ion, the C=N isomerization and ESIPT might be inhibited, leading to a fluorescence enhancement.

To further investigate the chemosensing properties of **1**, a fluorimetric titration of **1** was performed with the Zn^{2+} ion. As shown in Fig. 2, the emission intensity of **1** at 525 nm steadily increased until the amount of Zn^{2+} reached 15 equiv. The photophysical properties of **1** were also examined using UV-vis spectrometry. The UV-vis absorption spectrum of **1** showed a sharp band

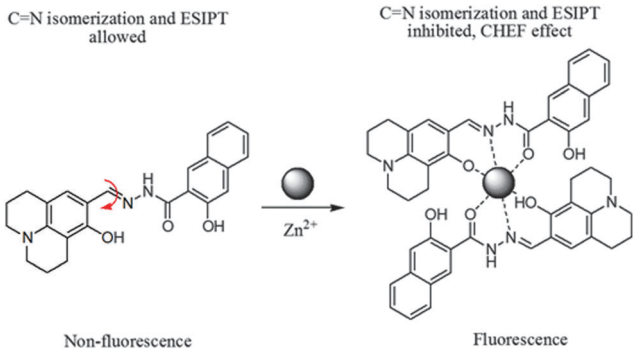

Scheme 2 Fluorescence enhancement mechanism and proposed structure of the Zn^{2+}–2·**1** complex.

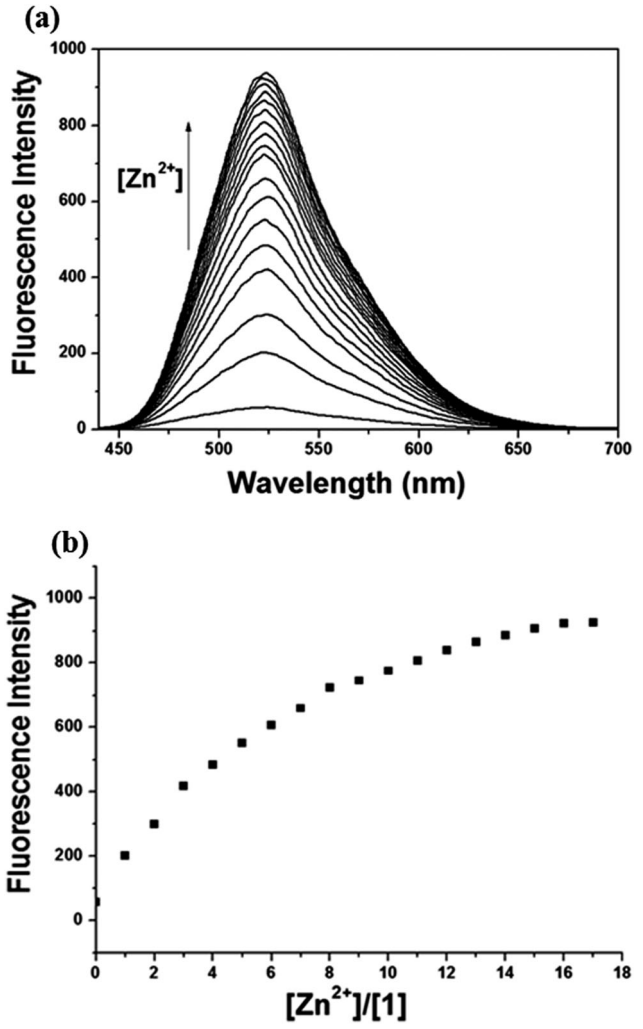

Fig. 2 (a) Fluorescence spectral changes of **1** (10 μM) in the presence of different concentrations of Zn^{2+} ions in buffer–DMF (1 : 1, v/v) solution. (b) Fluorescence intensity at 525 nm *versus* the number of equiv. of Zn^{2+} added.

at 400 nm (Fig. S1, ESI†). Upon the addition of Zn^{2+} ions to a solution of **1**, the absorption band at 400 nm has red-shifted to 425 nm. Meanwhile, two clear isosbestic points at 352 and 407 nm imply the undoubted conversion of free **1** to a zinc complex.

The Job plot[16] showed a 2 : 1 complexation stoichiometry between **1** and Zn^{2+} (Fig. S2, ESI†), which was further confirmed by ESI-mass spectrometry analysis (Fig. S3, ESI†). The positive-ion mass spectrum indicated that a peak at m/z = 865.00 is assignable to 2·**1** + Zn^{2+}–H^+ [calcd, m/z: 865.27]. Based on the Job plot and ESI-mass spectrometry analysis, we propose the structure of the Zn^{2+}–2·**1** complex, as shown in Scheme 2. From the fluorescence titration data, the association constant for Zn^{2+}–2·**1** complexation was determined to be 1.0×10^9 M^{-2} from Li's equations (Fig. S4, ESI†).[17] This value is in the range of those ($1.0–1.0 \times 10^{12}$) previously reported for Zn^{2+}-binding chemosensors.[10a,18] The detection limit[19] of receptor **1** as a fluorescence sensor for the analysis of Zn^{2+} ions was found to be 3.3×10^{-6} M (Fig. S5, ESI†). The detection limit of **1** is far below the WHO guidelines for drinking water (76 μM).[20]

To further check the practical applicability of receptor **1** as a Zn^{2+} selective fluorescent sensor, we carried out competition experiments. **1** was treated with 15 equiv. of Zn^{2+} in the presence of other metal ions of the same concentration. As shown in Fig. 3, other background metal ions had small or no obvious interference with the detection of Zn^{2+} ions, except for Cu^{2+}, Fe^{2+} and Co^{2+}. However, it is worth noting that cadmium ions hardly inhibited the fluorescence intensity of the Zn^{2+}–2·**1** complex. Hence, these results suggest that **1** could be a good sensor for Zn^{2+} and, in particular, distinguish Zn^{2+} from Cd^{2+} both having many common properties.[21]

Since the pH value affects the charge distribution of receptor **1** or may change its inherent fluorescence properties, the effect of pH on the emission bands of **1** in DMF/bis-tris buffer (1 : 1) solution was also studied (Fig. S6, ESI†). The Zn^{2+}–2·**1** complex showed a significant fluorescence response between pH 7 and 11, which includes the environmentally relevant range of pH 7.0–8.4.[22] These results indicate that Zn^{2+} could be clearly detected by the fluorescence spectral measurement using **1** within the environmental pH range (pH 7.0–8.4).

To examine the reversibility of receptor **1** toward Zn^{2+} in DMF/bis-tris buffer (1 : 1) solution, ethylenediaminetetraacetic

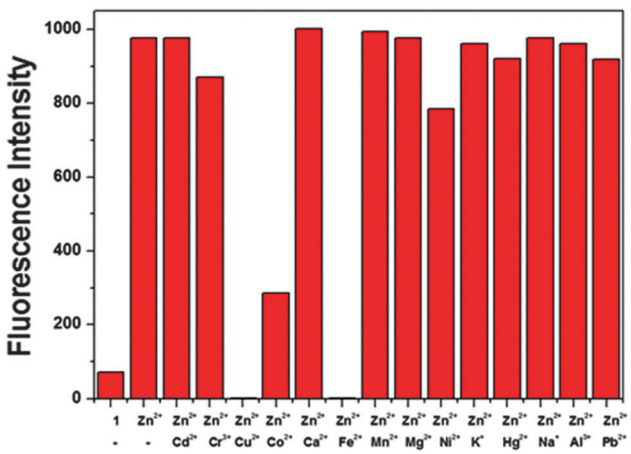

Fig. 3 Competitive selectivity of **1** (10 μM) toward Zn^{2+} (15 equiv.) in the presence of other metal ions (15 equiv.) with an excitation of 410 nm in buffer–DMF (1 : 1, v/v) solution.

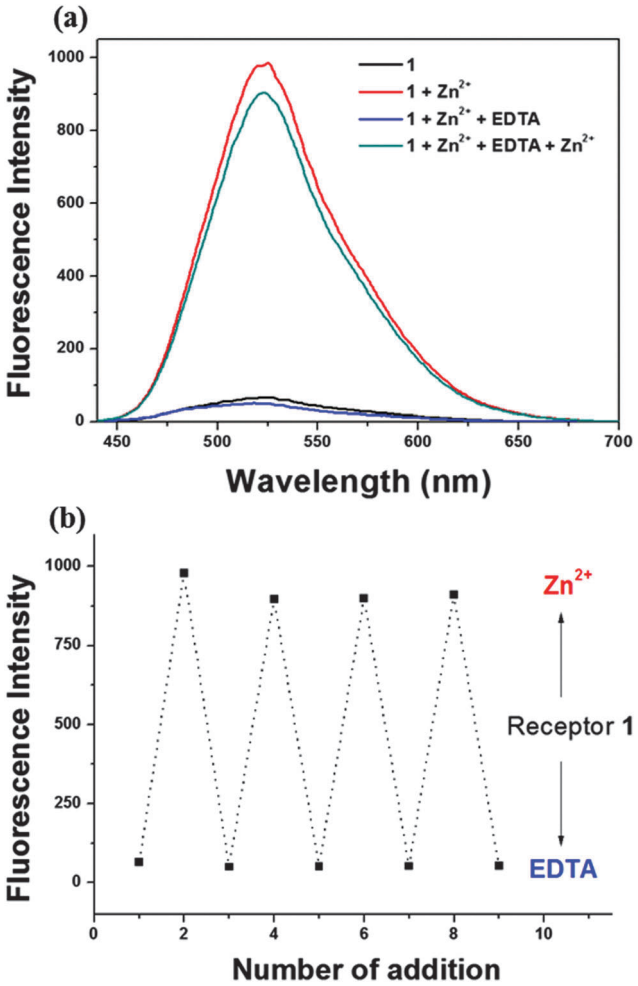

Fig. 4 (a) Fluorescence spectral changes of **1** (10 μM) after the sequential addition of Zn^{2+} and EDTA in buffer–DMF (1 : 1, v/v) solution. (b) Reversible changes in fluorescence intensity of **1** (10 μM) at 525 nm after the sequential addition of Zn^{2+} and EDTA.

acid (EDTA) (15 equiv.) was added to the complexed solution of receptor **1** and Zn^{2+}. As shown in Fig. 4, a fluorescence signal at 525 nm was completely quenched. Upon addition of Al^{3+} again, the fluorescence was recovered. The fluorescence emission changes were almost reversible even after several cycles with the sequentially alternative addition of Zn^{2+} and EDTA. These results indicate that the receptor **1** could be used as a reversible fluorescence chemosensor in aqueous solution.

In order to further examine the binding mode of **1** with Zn^{2+}, we have performed ^{1}H NMR titrations in DMSO-d_6 (Fig. 5). Upon addition of 0.5 equiv. of Zn^{2+}, the protons of amide (H_8) and imine (H_9) were downshifted by 0.012 and 0.003 ppm, respectively. Importantly, the proton of the julolidine OH moiety (H_{14}) underwent a slight chemical shift change, and then its integral value decreased to half. The halved proton integral indicates that only one of two receptor molecules of the Zn^{2+}–2·**1** complex is deprotonated, and this observation is consistent with the ESI-mass spectrometry analysis. The proton (H_1) did hardly change, suggesting that the oxygen atoms of the naphthol moieties might not be involved in Zn^{2+} coordination.

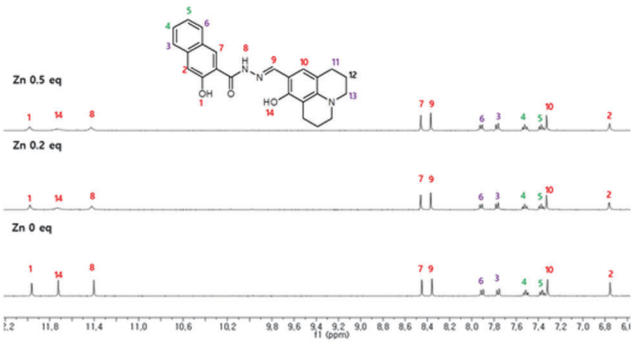

Fig. 5 ^{1}H NMR titration of **1** with $Zn(NO_3)_2$ in DMSO-d_6.

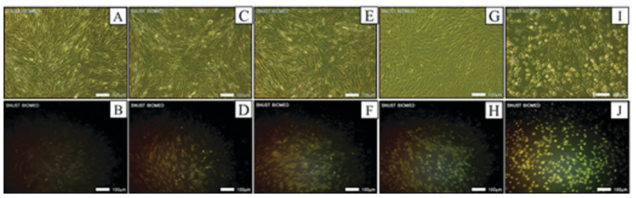

Fig. 6 Fluorescence images of fibroblasts cultured with Zn^{2+} and **1**. Cells were exposed to 0 (A and B), 10 (C and D), 20 (E and F), 40 (G and H) and 50 (I and J) μM $Zn(NO_3)_2$ for four hours and then later with **1** (20 μM) for 30 min. The top images (A, C, E, G, and I) were observed using a light microscope and the bottom images were taken using a fluorescence microscope. The scale bar is 100 μm.

Therefore, the ^{1}H NMR titration results support the structure of a 2 : 1 complex of **1** and Zn^{2+} proposed by the Job plot and ESI-mass spectrometry analysis (Scheme 2).

To further demonstrate biological application of **1**, fluorescence imaging experiments were carried out in living cells (Fig. 6). Adult human dermal fibroblasts were first incubated with various concentrations of aqueous Zn^{2+} solutions (0, 10, 20, 30, 40, and 50 μM) for 4 h and then exposed to **1** (20 μM) for 30 min before imaging. The fibroblast cells without either Zn^{2+} or **1** showed negligible intracellular fluorescence. However, the cells cultured with both Zn^{2+} and **1** exhibited fluorescence. The fluorescence intensity of the cells with **1** increased, with an increase in Zn^{2+} concentration from 10 to 50 μM. These results confirm that **1** can be a suitable sensor to detect Zn^{2+} in living cells.

Fluorescence and absorption spectroscopic studies of 1 toward acetate

In addition to the metal-ion sensing properties, we also investigated the fluorescence behavior of **1** toward different anions (F^-, Cl^-, Br^-, I^-, OAc^-, N_3^-, $H_2PO_4^-$ and CN^-) in DMF. Upon the addition of 100 equiv. of each anion to **1**, it was observed that among all, only F^- and OAc^- resulted in a drastic enhancement of the emission intensity of **1**, while other anions showed no or slight increase in the fluorescence spectra relative to that of the pure receptor **1** at 525 nm with excitation at 410 nm (Fig. 7a).

Next, we increased percent of water to **1** in DMF in order to examine a practical application. The best selectivity for acetate was observed in a mixture of DMF : water (v/v, 7 : 3). Upon the addition of 100 equiv. of each anion to **1** in the DMF–water

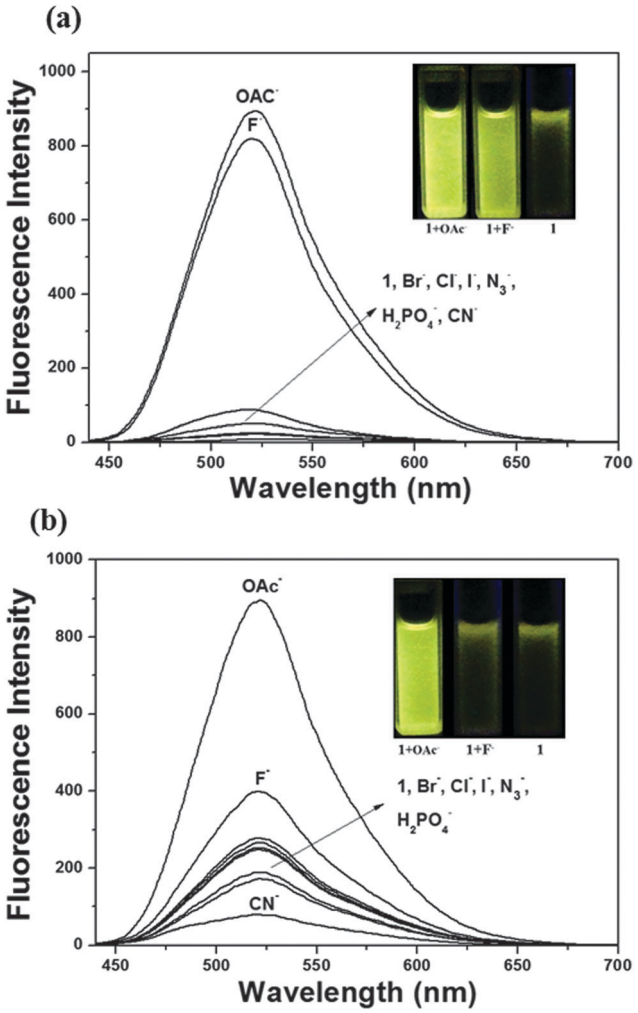

Fig. 7 (a) Fluorescence spectral changes of **1** (10 μM) in the presence of different anions (100 equiv.) such as F^-, Cl^-, Br^-, I^-, CN^-, N_3^-, $H_2PO_4^-$ and OAc^- with an excitation of 410 nm in DMF solution. (b) Fluorescence spectral changes of **1** (10 μM) in the presence of different anions (100 equiv.) with an excitation of 410 nm in buffer–DMF (7 : 3, v/v) solution.

mixture, only OAc^- resulted in a drastic enhancement of the emission intensity with quantum yield (Φ = 0.260), while other anions including F^- showed slight or no increase in the fluorescence spectra relative to the free receptor **1** with quantum yield (Φ = 0.0686) at 525 nm with excitation at 410 nm (Fig. 7b). This is possibly due to the preference of a strong chelating effect between **1** and the acetate over hydrogen bonding between water molecules and basic anions. Both F^- and OAc^- form hydrogen bonds to the phenolic and amide protons in **1**. In aprotic solvents like DMF, **1** showed selectivity toward both OAc^- and F^- (Fig. 7a). However, in the presence of a protic solvent, like water, F^- is more prone to form H-bond with water than with **1**.[23,24] On the other hand, OAc^-, behaving as a bidentate ligand, forms stable chelate like complexes through the protons of receptor **1**, (Scheme 3), thereby, forming $\mathbf{1}^{3-}$ species, having a strong fluorescence feature.[25]

The recognition ability of **1** for OAc^- was investigated by fluorescence titration, as shown in Fig. 8a. The emission

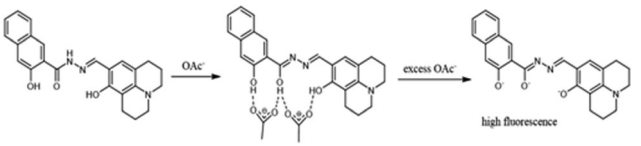

Scheme 3 Fluorescent enhancement mechanism of receptor **1** with OAc^-.

intensity of **1** at 525 nm steadily increased until the amount of OAc^- reached 100 equiv. (Fig. 8b). The photophysical properties of **1** were also examined using UV-vis spectrometry. UV-vis spectrum of **1** exhibited a sharp absorption band at 400 nm (Fig. S7, ESI†). Upon the addition of OAc^- to a solution of **1**, the absorption band at 400 nm has red-shifted to 415 nm, accompanied by the formation of two isosbestic points at 360 and 408 nm.

The Job plot showed a 1 : 2 stoichiometry between **1** and OAc^- (Fig. S8, ESI†). From the fluorescence titration data, the association constant for **1** with OAc^- was determined to be $2.6 \times 10^5\ M^{-2}$ using Li's equations (Fig. S9, ESI†). This value is

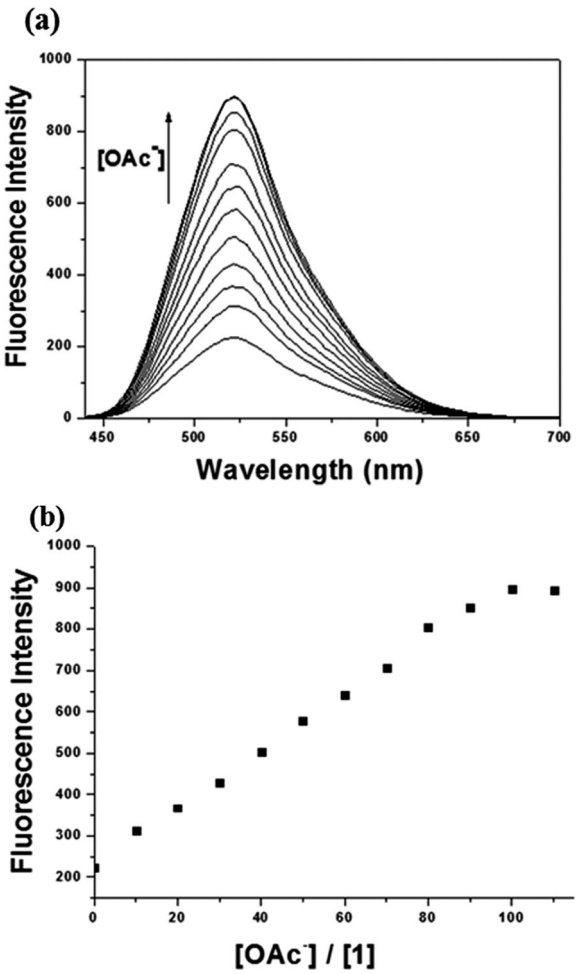

Fig. 8 (a) Fluorescence spectral changes of **1** (10 μM) in the presence of different concentrations of OAc^- ions (100, 200, 300, 400, 500, 600, 700, 800, 900, 1000 and 1100 μM) in buffer–DMF (7 : 3, v/v) solution at room temperature. (b) Fluorescence intensity at 525 nm *versus* equivalents of OAc^- added.

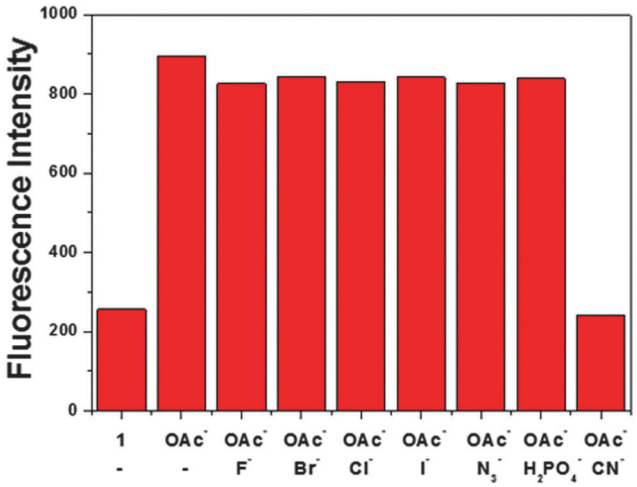

Fig. 9 Competitive selectivity of **1** (10 μM) towards OAc^- (100 equiv.) in the presence of other anions (100 equiv.) in buffer–DMF (7 : 3, v/v) solution.

within the range of those (1.0×10^2–6.0×10^5) reported for the acetate ion-recognition chemo-sensors.[5b,c,26] The detection limit of receptor **1** as a fluorescence sensor for the analysis of OAc^- ions was found to be 8.2×10^{-7} M (Fig. S10, ESI†). The preferential selectivity of **1** as a fluorescence chemosensor for the detection of acetate ions was studied in the presence of various competing anions. For competition studies, receptor **1** was treated with 100 equiv. of OAc^- in the presence of 100 equiv. of other anions, as indicated in Fig. 9. There was no interference in the detection of OAc^- in the presence of F^-, Cl^-, Br^-, I^-, N_3^-, and $H_2PO_4^-$, while CN^- did interfere. Thus, **1** could be used as a selective fluorescence sensor for OAc^- in the presence of most of the competing anions.

To further understand the nature of interaction between sensor **1** and the acetate ion a ^1H NMR study was initiated in DMF-d_7 (Fig. 10). Upon addition of 1 equiv. of TBA(OAc) as the acetate ion source, the broad protons (H_1 and H_{14}) of naphthol and julolidine OH moieties were downshifted from 17.322 ppm to 17.458 ppm. The H_8 of the amide group in **1** was broadened and also induced a downfield chemical shift to 17.458 ppm. After the addition of 2 equiv. of acetate ions, all the broad protons (H_1, H_8 and H_{14}) disappeared. All aromatic protons were shifted to upfield, which suggested that the negative charges generated from the deprotonation of **1** by OAc^- were delocalized over the whole receptor molecule. No shift in the position of proton signals was observed upon any further addition of OAc^- (> 2.0 equiv.), confirming a 1 : 2 stoichiometry between **1** and the acetate ion (Scheme 3).

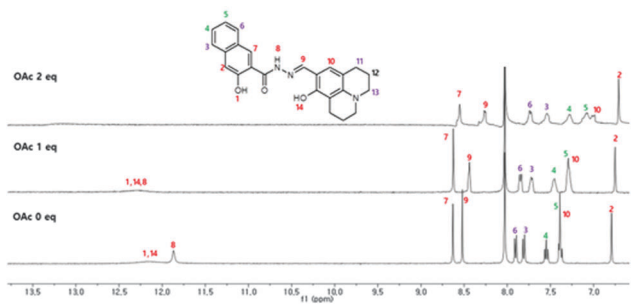

Fig. 10 ^1H NMR titration of **1** with TBA(OAc) in DMF-d_7.

Conclusions

We have synthesized a bifunctional fluorescence sensor based on the combination of 3-hydroxy-2-naphthoic hydrazide and 8-hydroxyjulolidine-9-carboxaldehyde. The receptor **1** exhibited a fluorescence enhancement upon binding to Zn^{2+} in aqueous solution due to a combinational effect of the inhibition of ESIPT and C=N isomerization, and CHEF. The binding of the receptor **1** and Zn^{2+} was also chemically reversible with EDTA. Moreover, *in vitro* studies with fibroblasts showed fluorescence when both sensor **1** and Zn^{2+} were present. Furthermore, **1** can selectively detect OAc^- among various anions *via* a fluorescence enhancement through deprotonation of **1** in aqueous media. These results provide a useful sensing strategy for the concept of 'a single chemosensor for multiple analytes'.

Acknowledgements

Basic Science Research Program through the National Research Foundation of Korea (NRF) funded by the Ministry of Education, Science and Technology (2012001725 and 2012008875) is gratefully acknowledged.

Notes and references

1 (*a*) K. K. Upadhyay and A. Kumar, *Org. Biomol. Chem.*, 2010, **8**, 4892–4897; (*b*) D. Karak, S. Lohar, A. Banerjee, A. Sahana, I. Hauli, S. K. Mukhopadhyay, J. S. Matalobos and D. Das, *RSC Adv.*, 2012, **2**, 12447–12454; (*c*) Y. J. Lee, D. Seo, J. Y. Kwon, G. Son, M. S. Park, Y. Choi, J. H. Soh, H. N. Lee, K. D. Lee and J. Yoon, *Tetrahedron*, 2006, **62**, 12340–12344; (*d*) M. Kumar, N. Kumar and V. Bhalla, *Dalton Trans.*, 2012, **41**, 10189–10193; (*e*) K. B. Kim, D. M. You, J. H. Jeon, Y. H. Yeon, J. H. Kim and C. Kim, *Tetrahedron Lett.*, 2014, **55**, 1347–1352.

2 (*a*) X. Chen, S. Nam, G. Kim, N. Song, Y. Jeong, I. Shin, S. K. Kim, J. Kim, S. Park and J. Yoon, *Chem. Commun.*, 2010, **46**, 8953–8955; (*b*) S. Kumar, V. Luxami and A. Kumar, *Org. Lett.*, 2008, **10**, 5549–5552; (*c*) V. Bhalla, S. Pramanik and M. Kumar, *Chem. Commun.*, 2013, **49**, 895–897.

3 (*a*) M. S. Park, K. M. K. Swamy, Y. J. Lee, H. N. Lee, Y. J. Jang, Y. H. Moon and J. Yoon, *Tetrahedron Lett.*, 2006, **47**, 8129–8132; (*b*) Z. Xu, G. Kim, S. J. Han, M. J. Jou, C. Lee, I. Shin and J. Yoon, *Tetrahedron*, 2009, **65**, 2307–2312; (*c*) J. Y. Choi, D. Kim and J. Yoon, *Dyes Pigm.*, 2013, **96**, 176–179; (*d*) O. A. H. Åstrand, L. P. E. Austdal, R. E. Paulsen, T. V. Hansen and P. Rongved, *Tetrahedron*, 2013, **69**, 8645–8654; (*e*) H. G. Lee, K. B. Kim, G. J. Park, Y. J. Na, H. Y. Jo, S. A. Lee and C. Kim, *Inorg. Chem. Commun.*, 2014, **39**, 61–65; (*f*) H. G. Lee, J. H. Lee, S. P. Jang, I. H. Hwang,

S. Kim, Y. Kim and C. Kim, *Inorg. Chim. Acta*, 2013, **394**, 542–551.

4 (*a*) Y. Li, Q. Zhao, H. Yang, S. Liu, X. Liu, Y. Zhang, T. Hu, J. Chen, Z. Chang and X. Bu, *Analyst*, 2013, **138**, 5486–5494; (*b*) Z. Xu, J. Yoon and D. R. Spring, *Chem. Soc. Rev.*, 2010, **39**, 1996–2006; (*c*) M. Yan, T. Li and Z. Yang, *Inorg. Chem. Commun.*, 2011, **14**, 463–465; (*d*) P. Jiang and Z. Guo, *Coord. Chem. Rev.*, 2004, **248**, 205–229; (*e*) H. Kim, J. Kang, K. B. Kim, E. J. Song and C. Kim, *Spectrochim. Acta, Part A*, 2014, **118**, 883–887; (*f*) V. Bhalla, H. Arora, A. Dhir and M. Kumar, *Chem. Commun.*, 2012, **48**, 4722–4724; (*g*) V. Bhalla and M. Kumar, *Dalton Trans.*, 2013, **42**, 975–980; (*h*) V. Bhalla and M. Kumar, *Org. Lett.*, 2012, **14**, 2802–2805; (*i*) V. Bhalla, V. Vij, M. Kumar, P. R. Sharma and T. Kaur, *Org. Lett.*, 2012, **14**, 1012–1015; (*j*) Y. W. Choi, G. J. Park, Y. J. Na, H. Y. Jo, S. A. Lee, G. R. You and C. Kim, *Sens. Actuators, B*, 2014, **194**, 343–352; (*k*) E. J. Song, H. Kim, I. H. Hwang, K. B. Kim, A. R. Kim, I. Noh and C. Kim, *Sens. Actuators, B*, 2014, **195**, 36–43.

5 (*a*) W. Huang, Y. Li, Z. Yang, H. Lin and H. Lin, *Spectrochim. Acta, Part A*, 2011, **79**, 471–475; (*b*) Y. Zhang, Q. Lin, T. Wei, D. Wang, H. Yao and Y. Wang, *Sens. Actuators, B*, 2009, **137**, 447–455; (*c*) S. Goswami, A. K. Das, K. Aich and A. Manna, *Tetrahedron Lett.*, 2013, **54**, 4215–4220.

6 (*a*) W. Huang, H. Su, H. Lin and H. Lin, *J. Inclusion Phenom. Macrocyclic Chem.*, 2011, **70**, 129–133; (*b*) W. Gong, B. Gao, S. Bao, J. Ye and G. Ning, *J. Inclusion Phenom. Macrocyclic Chem.*, 2012, **72**, 481–486; (*c*) A. Sola, A. Tárraga and P. Molina, *Dalton Trans.*, 2012, **41**, 8401–8409.

7 K. S. Rao, T. Balaji, T. P. Rao, Y. Babu and G. R. K. Naidu, *Spectrochim. Acta, Part B*, 2002, **57**, 1333–1338.

8 R. E. Sturgeon, S. S. Berman, A. Desaulniers and D. S. Russell, *Anal. Chem.*, 1979, **51**, 2364–2369.

9 R. Gulaboski, V. Mirčeski and F. Scholz, *Electrochem. Commun.*, 2002, **4**, 277–283.

10 (*a*) Y. Zhou, Z. Li, S. Zang, Y. Zhu, H. Zhang, H. Hou and T. C. W. Mak, *Org. Lett.*, 2012, **14**, 1214–1217; (*b*) E. J. Song, J. Kang, G. R. You, G. J. Park, Y. Kim, S. Kim, C. Kim and R. G. Harrison, *Dalton Trans.*, 2013, **42**, 15514–15520; (*c*) K. Hanaoka, Y. Muramatsu, Y. Urano, T. Terai and T. Nagano, *Chem. – Eur. J.*, 2010, **16**, 568–572; (*d*) H. G. Lee, J. H. Lee, S. P. Jang, H. M. Park, S. Kim, Y. Kim, C. Kim and R. G. Harrison, *Tetrahedron*, 2011, **67**, 8073–8078.

11 (*a*) H. Yang, H. Song, Y. Zhu and S. Yang, *Tetrahedron Lett.*, 2012, **53**, 2026–2029; (*b*) M. Kumar, N. Kumar and V. Bhalla, *Chem. Commun.*, 2013, **49**, 877–879; (*c*) S. Goswami, S. Das, K. Aich, D. Sarkar and T. K. Mondal, *Tetrahedron Lett.*, 2013, **54**, 6892–6896; (*d*) Z. Dong, X. Le, P. Zhou, C. Dong and J. Ma, *New J. Chem.*, 2014, **38**, 1802–1808; (*e*) D. Guo, Z. Dong, C. Luo, W. Zan, S. Yan and X. Yao, *RSC Adv.*, 2014, **4**, 5718–5725.

12 (*a*) X. Liu, N. Zhang, J. Zhou, T. Chang, C. Fang and D. Shangguan, *Analyst*, 2013, **138**, 901–906; (*b*) J. Wang, W. Lin and W. Li, *Chem. – Eur. J.*, 2012, **18**, 13629–13632; (*c*) J. H. Kim, J. Y. Noh, I. H. Hwang, J. Kang, J. Kim and C. Kim, *Tetrahedron Lett.*, 2013, **56**, 2415–2418; (*d*) Y. J. Na, I. H. Hwang, H. Y. Jo, S. A. Lee, G. J. Park and C. Kim, *Inorg. Chem. Commun.*, 2013, **35**, 342–345.

13 N. C. Lim, J. V. Shuster, M. C. Porto, M. A. Tanudra, L. Yao, H. C. Freake and C. Brückner, *Inorg. Chem.*, 2005, **45**, 2018–2030.

14 J. Wu, W. Liu, J. Ge, H. Zhang and P. Wang, *Chem. Soc. Rev.*, 2011, **40**, 3483–3495.

15 L. Wang, W. Qin, X. Tang, W. Dou and W. Liu, *J. Phys. Chem. A*, 2011, **115**, 1609–1616.

16 P. Job, *Ann. Chim.*, 1928, **9**, 113–203.

17 G. Grynkiewcz, M. Poenie and R. Y. Tsein, *J. Biol. Chem.*, 1985, **260**, 3440–3450.

18 (*a*) H. Y. Lin, P. Y. Cheng, C. F. Wan and A. T. Wu, *Analyst*, 2012, **137**, 4415–4417; (*b*) J. H. Kim, I. H. Hwang, S. P. Jang, J. Kang, S. Kim, I. Noh, Y. Kim, C. Kim and R. G. Harrison, *Dalton Trans.*, 2013, **42**, 5500–5507; (*c*) W. H. Hsieh, C. Wan, D. Liao and A. Wu, *Tetrahedron Lett.*, 2012, **53**, 5848–5851.

19 Y. K. Tsui, S. Devaraj and Y. P. Yen, *Sens. Actuators, B*, 2012, **161**, 510–519.

20 (*a*) Y. P. Kumar, P. King and V. S. K. R. Prasad, *Chem. Eng. J.*, 2006, **124**, 63–70; (*b*) K. B. Kim, H. Kim, E. J. Song, S. Kim, I. Noh and C. Kim, *Dalton Trans.*, 2013, **42**, 16569–16577.

21 L. Li, Y. Dang, H. Li, B. Wang and Y. Wu, *Tetrahedron Lett.*, 2010, **51**, 618–621.

22 R. M. Harrison, D. P. H. Laxen and S. J. Wilson, *Environ. Sci. Technol.*, 1981, **15**, 1378–1383.

23 H. Tavallali, G. D. Rad, A. Parhami and E. Abbasiyan, *Dyes Pigm.*, 2012, **94**, 541–547.

24 J. Li, T. Wei, Q. Lin, P. Li and Y. Zhang, *Spectrochim. Acta, Part A*, 2011, **83**, 187–193.

25 Y. Sun, Y. Liu, M. Chen and W. Guo, *Talanta*, 2009, **80**, 996–1000.

26 (*a*) S. Goswami, S. Maity, A. K. Das and A. C. Maity, *Tetrahedron Lett.*, 2013, **54**, 6631–6634; (*b*) W. Huang, Z. Chen, H. Lin and H. Lin, *J. Lumin.*, 2011, **131**, 592–596; (*c*) J. Shao, Y. Wang, H. Lin, J. Li and H. Lin, *Sens. Actuators, B*, 2008, **134**, 849–853; (*d*) X. Bao and Y. Zhou, *Sens. Actuators, B*, 2010, **147**, 434–441.

